

## **The Horizontal Magnetic Field of the Quiet Sun: Numerical Simulations in Comparison to Observations with Hinode**

O. Steiner, R. Rezaei, and R. Schlichenmaier

*Kiepenheuer-Institut für Sonnenphysik, 79104 Freiburg, Germany*

W. Schaffenberger

*Physics and Astronomy Department, Michigan State University, East  
Lansing MI 48824, USA*

S. Wedemeyer-Böhm

*Institute of Theoretical Astrophysics, P.O. Box 1029, Blindern, N-0316,  
Norway*

**Abstract.** Three-dimensional magnetohydrodynamic simulations of the surface layers of the Sun intrinsically produce a predominantly horizontal magnetic field in the photosphere. This is a robust result in the sense that it arises from simulations with largely different initial and boundary conditions for the magnetic field. While the disk-center synthetic circular and linear polarization signals agree with measurements from Hinode, their center-to-limb variation sensitively depends on the height variation of the horizontal and the vertical field component and they seem to be at variance with the observed behavior.

### **1. Introduction**

Observations with the spectropolarimeter of the Solar Optical Telescope (SOT) onboard the Hinode space observatory (Kosugi et al. 2007) indicate that seen with a spatial resolution of  $0.3''$ , quiet internetwork regions harbor a photospheric magnetic field whose mean field strength of its horizontal component considerably surpasses that of the vertical component (Lites et al. 2008; Orozco Suárez et al. 2007). According to these papers, the vertical fields are concentrated in the intergranular lanes, whereas the stronger, horizontal fields occur most commonly at the edges of the bright granules, aside from the vertical fields. Harvey et al. (2007) find from recordings with GONG and SOLIS a ‘seething magnetic field’ with a line-of-sight component increasing from disk center to limb as expected for a nearly horizontal field orientation. Ishikawa et al. (2008) detected transient horizontal magnetic fields in plage regions as well. Previously, Martínez Pillet et al. (1997) and Meunier et al. (1998) reported observations of weak and strong horizontal fields in quiet Sun regions.

Regarding numerical simulations, Grossmann-Doerth et al. (1998), note “we find in all simulations also strong horizontal fields above convective upflows”, and Schaffenberger et al. (2005, 2006) find frequent horizontal fields in their three-

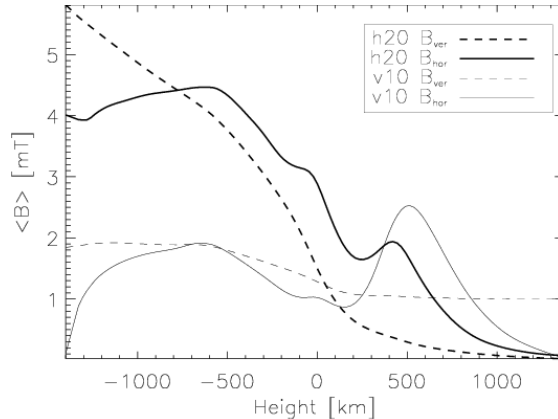


Figure 1. Horizontally and temporally averaged horizontal (solid) and vertical (dashed) absolute field strength as functions of height for run h20 (heavy curves) and for run v10 (light curves).

dimensional simulations, which they describe as “small-scale canopies”. Also the 3-D simulations of Abbett (2007) display “horizontally directed ribbons of magnetic flux that permeate the model chromosphere”, not unlike the figures shown by Schaffenberger et al. (2006). Schüssler & Vögler (2008) find in a three-dimensional surface-dynamo simulation “a clear dominance of the horizontal field in the height range where the spectral lines used for the Hinode observations are formed”.

Steiner et al. (2008) report on results from three-dimensional magnetohydrodynamic numerical simulations of the internetwork magnetic field with regard to the intrinsically produced horizontal magnetic field. They compute the polarimetric signal of this field and compare it to measurements with Hinode. In the following, we briefly summarize part of their results and present new calculations of the center-to-limb variation of the linear and circular polarization from these simulations.

## 2. Simulations

We have carried out three sets of numerical simulations, run v10, run h20, and run h50, which significantly differ in their initial and boundary conditions for the magnetic field. Run v10 starts with a homogeneous vertical field of 10 G strength, which is kept vertical at the top and bottom boundary. These conditions might actually be more appropriate for network magnetic fields because of the preference for one polarity and the vertical direction. Run h20 and run h50 start without a magnetic field but upwellings that enter the simulation domain across the bottom boundary area carry horizontal magnetic field of a uniform strength of 20 G and 50 G, respectively, into the box. The three-dimensional computational domain extends from 1400 km below the mean surface of optical depth  $\tau_c = 1$  to 1400 km above it, high enough that the top boundary condition should not unduly tamper the formation layers of the spectral lines that are used in polarimetric measurements with Hinode.

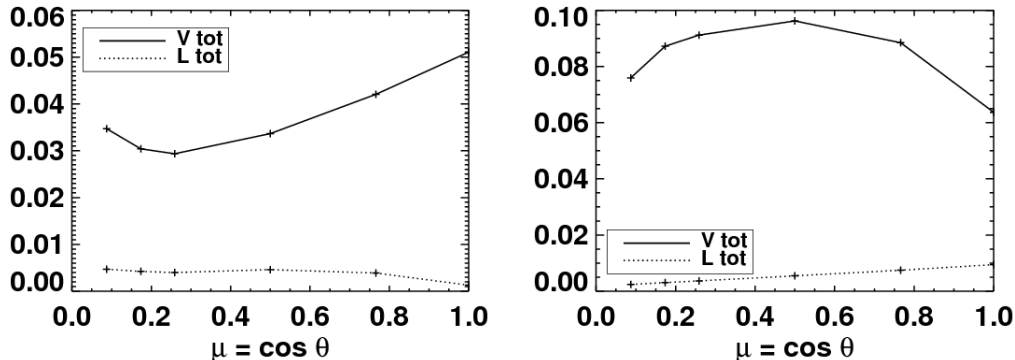


Figure 2. Center-to-limb variation (right to left) of the total (wavelength integrated) circular ( $V_{\text{tot}}$ ) and linear ( $L_{\text{tot}}$ ) polarization in pm of the Fe I 630.25 nm spectral line of a snapshot of run v10 (left) and h50 (right).

Figure 1 shows the horizontally and temporally averaged absolute vertical and horizontal magnetic field strength as functions of height of the magnetic field, which emerges from the two runs v10 and h20. In run h20, the mean horizontal field strength is larger than the mean strength of the vertical component throughout the photosphere and the lower chromosphere: in run v10 this is the case in the height range between 250 km and 850 km. Both runs show a local maximum in the horizontal field strength close to the classical temperature minimum at a height of around 500 km. At a given continuum optical depth in the photosphere the area occupied by fields with a horizontal component stronger than a given threshold of a few gauss is typically three times larger than the area with a vertical component exceeding this limit.

For a comparison with Zeeman measurements from the Hinode spectropolarimeter we synthesized the Stokes profiles of both 630 nm Fe I spectral lines of the two simulation runs. Profiles were computed with the radiative transfer code SIR (Ruiz Cobo & del Toro Iniesta 1992) with a spectral sampling of 2 pm. When applying an appropriate point spread function, PSF, (Wedemeyer-Böhm 2008) to the synthetic profiles and subjecting them to the same procedure for conversion to apparent flux densities as done by Lites et al. (2008) for the observed profiles, we obtain spatial and temporal averages for the transversal and longitudinal apparent magnetic flux densities,  $B_{\text{app}}^{\text{T}}$  and  $|B_{\text{app}}^{\text{L}}|$  of respectively  $21.5 \text{ Mx cm}^{-2}$  and  $5.0 \text{ Mx cm}^{-2}$  for run h20 and  $10.4 \text{ Mx cm}^{-2}$  and  $6.6 \text{ Mx cm}^{-2}$  for run v10. Thus, the ratio  $r = \langle B_{\text{app}}^{\text{T}} \rangle / \langle |B_{\text{app}}^{\text{L}}| \rangle = 4.3$  for h20 and 1.6 for v10. Lites et al. (2008) obtain from Hinode SP data  $\langle |B_{\text{app}}^{\text{T}}| \rangle = 55 \text{ Mx cm}^{-2}$  and  $\langle |B_{\text{app}}^{\text{L}}| \rangle = 11 \text{ Mx cm}^{-2}$  resulting in  $r = 5.0$ .

### 3. Center-to-limb variation (CLV)

Figure 2 shows the center-to-limb variation of the wavelength integrated absolute circular ( $V_{\text{tot}}$ ) and absolute linear ( $L_{\text{tot}}$ ) polarization signal, for the 630.25 nm Fe I spectral line in pm. The left panel of Fig. 2 shows the result for run v10, the right panel for run h50, both for one single simulation snapshot. For these results

foreshortening was taken into account but no PSF. The computational domain of h50 is in the horizontal directions twice as large as that for v10 and h20. The CLV of  $V_{\text{tot}}$  and  $L_{\text{tot}}$  substantially differ between v10 and h50, which indicates that they sensitively depend on the precise height variation of the horizontal and the vertical component of the magnetic field. Since the vertical component of v10 dominates over the horizontal one in the low photosphere (cf. Fig. 1), the mean longitudinal (line-of-sight) field component decreases when moving away from disk center and only when approaching the limb it increases again due to the sharp increase of the horizontal component above  $z \approx 200$  km. This behavior is reflected in the CLV of  $V_{\text{tot}}$  of run v10. The transversal component, viz. the component perpendicular to the line-of-sight and hence  $L_{\text{tot}}$ , increases at first because the vertical component stays almost constant with height in model v10 (in contrast to model h20 or h50). For h50 we have an increase in the longitudinal component as a function of disk-center distance because the horizontal component dominates throughout the photosphere and as a consequence, the transversal component decreases. This behavior is reflected by the CLV of  $V_{\text{tot}}$  and  $L_{\text{tot}}$  of run h50.

While the CLV of Fig. 2 finds a natural explanation in terms of the vertical structure of  $\langle B_{\text{hor}} \rangle$  and  $\langle B_{\text{ver}} \rangle$  shown in Fig. 1, the observations by Lites et al. (2008) tell a different story. Accordingly, the circular polarization signal decreases from the disk center to the limb as it does in Fig. 2 (left). But also the linear polarization signal decreases like in Fig. 2 (right). None of the two simulation snapshots to which Fig. 2 refers show a simultaneous and monotonic decrease in both quantities.

## References

- Abbett, W. P. 2007, *ApJ*, 665, 1469
- Grossmann-Doerth, U., Schüssler, M., & Steiner, O. 1998, *A&A*, 337, 928
- Harvey, J. W., Branston, D., Henney, C. J., & Keller, C. U. 2007, *ApJ*, 659, L177
- Ishikawa, R., Tsuneta, S., Ichimoto, K., Isobe, H., Katsukawa, Y., et al. 2008, *A&A*, 481, L25
- Kosugi, T., Matsuzaki, K., Sakao, T., Shimizu, T., Sone, Y., et al. 2007, *Solar Phys.*, 243, 3
- Lites, B. W., Kubo, M., Socas-Navarro, H., Berger, T., Frank, Z., et al. 2008, *ApJ*, 672, 1237
- Martínez Pillet, V., Lites, B. W., & Skumanich, A. 1997, *ApJ*, 474, 810
- Meunier, N., Solanki, S. K., & Livingston, W. C. 1998, *A&A*, 331, 771
- Berger, T., Orozco Suárez, D., Bellot Rubio, L. R., del Toro Iniesta, J. C., Tsuneta, S., Lites, B. W., et al. 2007, *ApJ*, 670, L61
- Ruiz Cobo, B., & del Toro Iniesta, J. C. 1992, *ApJ*, 398, 375
- Schaffenberger, W., Wedemeyer-Böhm, S., Steiner, O., & Freytag, B. 2005, in *ESA Special Publication*, Vol. 596, *Chromospheric and Coronal Magnetic Fields*, ed. D. E. Innes, A. Lagg, & S. A. Solanki
- Schaffenberger, W., Wedemeyer-Böhm, S., Steiner, O., & Freytag, B. 2006, in *ASP Conference Series*, Vol. 354, *Solar MHD Theory and Observations*, ed. J. Leibacher, R. F. Stein, & H. Uitenbroek, 345
- Schüssler, M., & Vögler, A. 2008, *A&A*, 481, L5
- Steiner, O., Rezaei, R., Schaffenberger, W., & Wedemeyer-Böhm, S. 2008, *ApJ*, 680, L85
- Wedemeyer-Böhm, S. 2008, *A&A*, 487, 399